Computational Analysis of Soft Polymer Lattices for 3D Wound Dressing Materials

Muhammad Hanif Nadhif [1,2], Muhammad Irsyad[2], Muhammad Satrio Utomo[1,2] , Muhammad Suhaeri[2,4], Yudan Whulanza [5,6]*

[1]Department of Medical Physics, Faculty of Medicine, Universitas Indonesia, Indonesia

[2]Medical Technology Cluster, Indonesia Medical Education and Research Institute (IMERI), Indonesia

[3]Research Center for Metallurgy and Material, Indonesia Institute of Science (LIPI), Indonesia

[4]Indonesia Unit of Education, Research, and Training, Universitas Indonesia Hospital, Universitas Indonesia, Indonesia

[5]Department of Mechanical Engineering, Faculty of Engineering, Universitas Indonesia

[6]Research Center on Biomedical Engineering (RCBE), Faculty of Engineering, Universitas Indonesia
**yudan@eng.ui.ac.id*

ABSTRACT

One of the wound treatments was negative pressure wound therapy (NPWT), which used wound dressings on the wound bed to ameliorate the wound healing. Unfortunately, most wound dressings were two dimensional (2D), lacking the ability to cover severe wounds with a straightforward procedure. The sheets needed to be stacked following the wound curvature, which might be problematic since improper stacking could hinder the wound healing. Regarding the mentioned problems, our group develop 3D wound dressings, which are made using 3D printers. The wound dressings are made of polycaprolactone (PCL), polyurethane (PU), and polyvinyl alcohol (PVA). As the initial stage, the mechanical integrity of the soft polymers was investigated

ISSN 1823-5514, eISSN 2550-164X

Received for review: 2020-11-16
Accepted for publication: 2021-02-04
Published: 2021-04-15

under uniaxial tensile and uniaxial compressive stress using computational methods. The polymers were defined as 3D lattices following the dimension of existing wound dressings. Based on the simulation results of displacement and von Mises stress, the three polymers are mechanically safe to be used as wound dressing materials.

Keywords: *Computational analysis; Lattice; Soft polymer; Wound dressing*

Introduction

Chronic ulcers affected 1% of the world population with various causes [1]. At least three types of chronic ulcer were known, venous leg ulcer, diabetic ulcer, and pressure ulcer. In Germany, 37% - 80% of leg ulcer cases had an aetiology of chronic venous insufficiency [2]. In the UK, venous ulcer prevalence could reach 1.2 – 3.2 per 1,000 people [3]. Apart from venous leg ulcers, diabetic foot ulcers also showed high prevalence. The incidence of diabetic foot ulcers also grown globally [4], along with the increase in the prevalence of diabetic mellitus all over the world. This type of ulcer was responsible for more hospitalization than other diabetic complications. This ulcer also increased the chance of the patient experiencing pressure ulcers [5]. Regardless of the diabetic co-factor, pressure ulcers also presented high prevalence, particularly in immobilized patients. It was reported that 18.1% of hospitalized patients in Europe were affected by pressure ulcers4. Both diabetic and pressure ulcers spent a high expenditure on national healthcare [4], [6].

The treatment of abovementioned ulcers varied. For the initial stage, the ulcer was cleansed using irrigation to remove debris and prevent premature surface healing [7]. The shallow ulcer usually only required wound dressing to close the ulcer and prevent contamination. However, higher-stage ulcers required a negative pressure wound therapy (NPWT) to accelerate the wound healing process by providing an electrically powered vacuum condition in the wound vicinity [8]. The vacuum condition enabled humidity maintenance, allowed for epithelization, and prevented tissue desiccation [9]. Due to the vacuum condition, the exudate could also be removed, thereby preventing contamination and lowering the risk of hematoma and seroma formation [10].

The selection of wound dressing for NPWT devices was crucial. Ulcers could react differently to different materials of wound dressing. To date, polycaprolactone (PCL), polyurethane (PU) dan polyvinyl alcohol (PVA) were regularly used as building blocks of wound dressings due to the biocompatibility [11]–[14]. Besides that, the use of materials was based on the softness since the materials interacted with damage skins (ulcers) [15], [16].

The available wound dressing materials, nonetheless, are mostly two dimensional (2D), in the form of sheet. For Stage III or Stage IV ulcers, the

2D wound dressing sheets have to be stacked to fill the gap in the wound cavity since every chronic ulcer had its own curvature. Sometimes, the wound dressing sheet was not able to fit properly in the wound bed, which caused the air leakage [17]. A loose stacking might cause a partially covered wound bed, while a tight stacking might induce pain to the wound bed. An improper stacking might also interfere with the vacuum perseverance of the NPWT. Regarding this problem, our group developed a three-dimensional (3D) wound dressing made of soft polymers. The 3D curvature of the wound dressing was extracted from medical imaging (i.e., magnetic resonance imaging, 3D scanning). The medical images were subsequently modified to generate a lattice pattern in the wound dressing, following the size of the existing wound dressing. The modified lattice-structured wound dressing was subsequently realized using rapid prototyping technology, as known as 3D printing.

Before the wound dressing realization, one of the crucial steps is the computational and experimental characterization of the wound dressing materials. This study aims to investigate the mechanical integrity of the materials using computational methods under several modes of stress. The materials were as 3D lattices made of soft polymers: PCL, PU, and PVA.

Methods

3D soft polymer lattice model

The model of the three lattices (PCL, PU, and PVA) was designed with the pore-strut configuration using an Autodesk Inventor Professional 2020 modelling software. The strut dimension was based on the maximum resolution of the 3D printer [18] and the setting in the slicer software. Low-cost fused deposition modelling (FDM) 3D printers commonly used a nozzle with a diameter of 0.4 mm [18]. The nozzle diameter determined the extrusion width (strut width), which had the same value as the nozzle diameter. The strut height, on the other hand, could be altered using a slicer software by choosing the 3D printing quality, which was the layer height per print. Commonly, the slightest dimension of the layer was 0.1 mm [18], thereby the strut height. From the mentioned considerations, the strut width and height were 0.4 mm and 0.1 mm, respectively. Different from the strut, which size was fixed, the pore dimension varied following the wound dressing specification applied in the NPWT device. There were three sizes of pore in literature: 0.4 mm [19], 0.5 mm [19], and 0.68 mm [20], thus generating three samples for each material, which had the same strut dimension, as well as the number of pores and struts. As a result, there were 9 samples: PCL0.68, PCL0.5, PCL0.4, PU0.68, PU0.5, PU0.4, PVA0.68, PVA0.5, and PVA0.4 The illustration of the 3D lattice is presented in Figure 1.

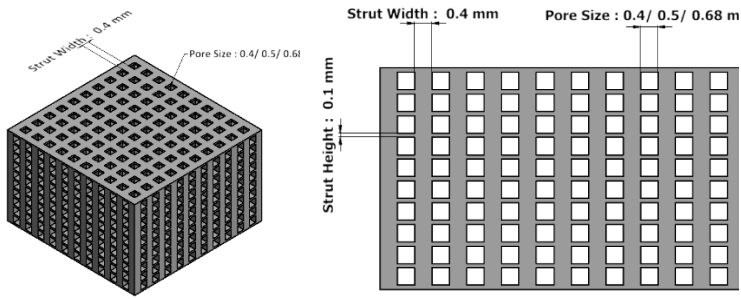

(a) (b)

Figure 1: The computer-aided design (CAD) of the soft polymer lattice: (a) isometric projection, and (b) front view of the model.

Simulation parameters

COMSOL Multiphysics 4.5 was used to perform the computational simulations to determine the mechanical integrity of the 3D lattice [21]. The model that was built (Figure 1) was converted and exported to COMSOL. In this study, the uniaxial compressive and tensile stresses were applied on top of the lattice surface. The simulations were performed using a solid mechanics module in the stationary study. The mechanical properties of the three materials input in COMSOL were in the form of thermoplastics, following the form of the 3D printing filaments (presented in Table 1).

Table 1: Mechanical properties of PCL, PU, and PVA

Parameters	PCL	PU	PVA
Young's Modulus (MPa)	Compressive: 44 [22] Tensile: 27 [22]	55 [23]	44.7 [24]
Poisson's Ratio	0.442 [22]	0.48 [23]	0.45 [25]
Density (kg/m3)	1,200 [26]	1,100 [27]	680 [28]
Tensile / Compressive Strength (MPa)	Compressive: 3.2 [22] Tensile: 1.4 [22]	24.8 [29]	40 [30]

The load boundary and fixed constraint were defined on two surfaces of the model. One was on top of the model, while the other one was applied on the bottom surface of the model, respectively. The load directed downward and upward along the z-axis placed on top of the model, recapitulated the compressive and tensile stress, respectively. To determine the value of the two forces, the working pressure of an NPWT device was used. On a clinical basis,

a 125-mmHg negative pressure was delivered to the wound bed [19]. Considering the safety factor of 10, the load used in this study was equal to 1250 mmHg (166,653 Pa). These simulations output resulted in the displacement and the von Mises Stress (vMS) of each material, model, and test used. The minimum-maximum value distribution of displacement was visualized by the colour scale (Figure 2). Following is the linear deformation equation:

$$\delta = \frac{PL}{EA} \tag{1}$$

where P, L, E, and A are the load (N), the original length of the lattice (mm), modulus elasticity of the material (N/mm2), and surface area (mm2), respectively. Meanwhile, the vMS calculation followed the below equation:

$$\sigma_V = \frac{1}{6}[(\sigma_{11} - \sigma_{22})^2 + (\sigma_{22} - \sigma_{33})^2 + (\sigma_{33} - \sigma_{11})^2] + \sigma_{12}^2 + \sigma_{23}^2 + \sigma_{31}^2 \tag{2}$$

where σij is the stress tensor at the local coordinate system.

Results and Discussion

The displacement values were analysed using a COMSOL post-processing feature and evaluated from the top surface. Since the working force was on the z-axis, the displacement values along other axes were neglected. The simulation in COMSOL followed Equation 1. In all the samples, the lowest displacement values were distributed on all four corners on the bottom surface. Meanwhile, the higher displacement values were found on the middle surface, especially at the edges of the pores. The distribution values were visualized in Figure 2.

The resulted displacement values were obtained regarding the test method, pore size, and material were summarized in Figure 3a. The displacement increased along with the increase of the pore size. For both tensile and compressive tests, PU models had the lowest displacement among all materials in all pore sizes. The displacement values were 0.048 mm, 0.083 mm, and 0.129 mm for PU0.4, PU0.5, PU0.68, respectively. Meanwhile, the displacement values of the PVA0.4, PVA0.5, PVA0.68 model were 0.06 mm, 0.104 mm, and 0.161 mm, respectively. The PCL model for both test schemes had distinctive displacement values due to the difference of compressive and tensile strength. The compressive displacements of PCL0.4, PCL0.5, and PCL0.68 were 0.061 mm, 0.106 mm, and 0.164 mm, respectively. Meanwhile,

the tensile displacements of PCL0.4, PCL0.5, and PCL0.68 were 0.1 mm, 0.173 mm, 0.267 mm, respectively.

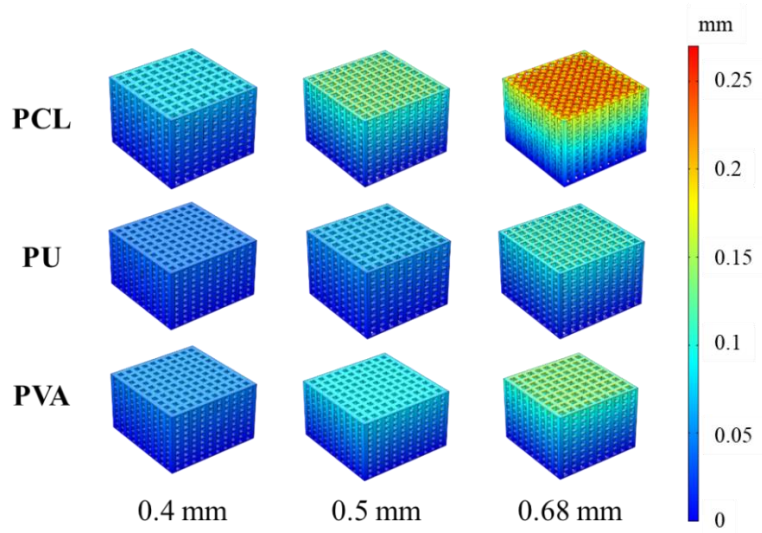

Figure 2: Displacement distribution on tensile test for each pore size and material.

Generally, the PU lattice has the lowest displacement in the compressive and tensile tests, followed by PVA and PCL (dPU < dPVA < dPCL). The displacement results inversely corresponded to the elastic modulus of each material (EPU > EPVA > EPCL), as shown in Table 1. The results also indicated that the PU lattice was more stable to preserve its shape compared with the PVA and PCL lattices. However, despite the highest displacement of PCL, the maximum tensile strain was only about 3.38%. This small strain can be considerably neglected during the implementation of NPWT.

The vMS values were also obtained from the simulation (Figure 3b), following Equation 2. The average vMS values were 1.21 ± 0.01 MPa, 2.02 ± 0.01 MPa, and 3.36 ± 0.06 MPa for the pore size of 0.4 mm, 0.5 mm, 0.68 mm, respectively. The simulation indicated that for the same strut size, the resulted vMS for each material was proportional to the pore size. The vMS values were lower than the respective ultimate tensile strength (UTS) values (shown in Table 1), except for the PCL lattice with the pore size of 0.5 mm and 0.68 mm. In terms of compressive stress, only vMS of PCL with the pore size of 0.68 mm exceeded the ultimate compressive strength (UCS). The three explained conditions were indeed problematic since the conditions indicated the failure

of materials. However, the safety factor used in the simulation was overestimated, 10. When the safety factor was lowered to 5 (P= 83, 326 Pa), the vMS of the PCL lattice with the pore size of 0.5 mm was lower than the UTS. When the safety factor was even decreased to 4 (P= 66, 661 Pa), the PCL lattice with the pore size of 0.68 mm did not experience failure due to either tensile or compressive stress. These results are of importance for the future design of 3D wound dressings made of PCL. Instead of 10, the safety factor used for PCL wound dressings can be 4. The safety factor of 4 is still tolerable.

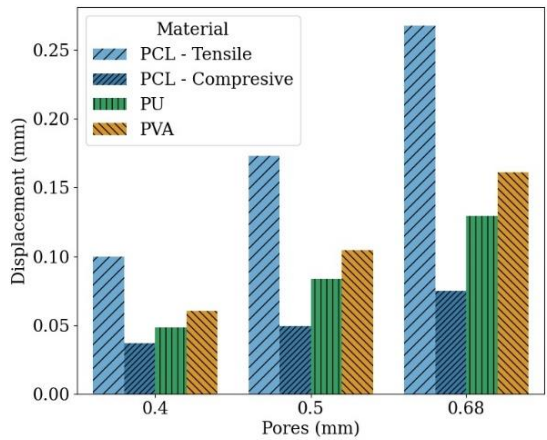

(a)

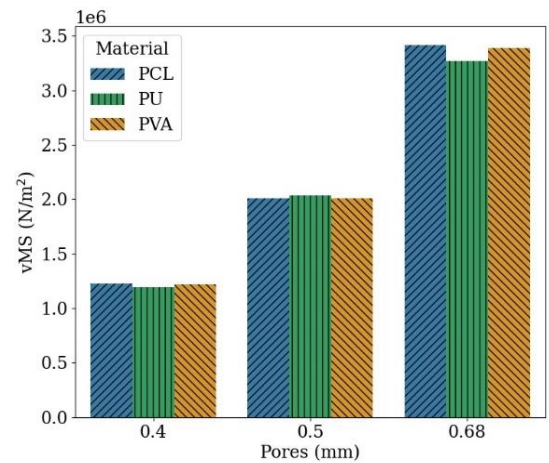

(b)

Figure 3: Displacement (a) von Mises Stress, and (b) along the z-axis.

Based on the mechanical simulation results, the 3D PU lattice was superior compared to the other two lattices. However, the strain of all lattices was very small (Table 2). The vMS of all materials was below the UTS, except for PCL with certain pore sizes. Nonetheless, when the safety factor was lowered to 4, PCL lattices were still safe and applicable for NPWT. It means that the other two materials (PVA and PCL) can still be considered as compatible materials for NPWT wound dressings. Therefore, three options of 3D wound dressing material are still available for plastic surgeons to use. For instance, if the surgeons would like to incorporate a biodegradable wound dressing, they can select 3D PVA-based and PCL-based wound dressings [31]–[33]. Meanwhile, when the surgeons want to keep the structural integrity of the 3D wound dressing material, they can choose 3D PU-based wound dressing since thermoplastic PU is not degradable in the body [13].

Table 2: The strain for each pore size and material

Material	Pore Size		
	0.4 mm	0.5 mm	0.68 mm
PCL (%)	1.95	2.84	3.39
PU (%)	0.95	1.37	1.64
PVA (%)	1.18	1.71	2.04

Conclusion

The computational analysis was successfully executed. From the results, it can be concluded that the 3D lattices made of PCL, PU, and PVA, were safe and feasible to be used as wound dressing materials. The von Mises stress resulted from the equivalent stress produced by NPWT devices on a wound bed did not exceed the ultimate tensile strength of all materials. The maximum strain rate due to the compressive and tensile stress was also considerably low. In terms of biodegradability, surgeons can take 3D PVA- and PCL-based wound dressings. On the other hand, the perseverance of 3D wound dressing structural integrity can be achieved using PU-based wound dressings. Finally, the results of this study provide the readers the finite element analysis of 3D lattices for wound dressing applications. However, this study hopefully will become a cornerstone of the development of 3D wound dressing materials, experimentally and clinically, since a one-piece dressing product was desired by burn wound specialists around the world [34].

Acknowledgement

This research was supported by the Universitas Indonesia through the PUTI Saintekes Grant NKB-2444/UN2.RST/HKP.05.00/2020.

References

[1] L. Martinengo *et al.*, "Prevalence of chronic wounds in the general population: systematic review and meta-analysis of observational studies," *Ann. Epidemiol.*, vol. 29, pp. 8–15, 2019.

[2] K. Heyer, K. Protz, G. Glaeske, and M. Augustin, "Epidemiology and use of compression treatment in venous leg ulcers: nationwide claims data analysis in Germany: Compression treatment in venous leg ulcers," *Int. Wound J.*, vol. 14, no. 2, pp. 338–343, 2017.

[3] A. H. Davies, J. M. Mora, M. S. Gohel, F. Heatley, and K. Dhillon, "Early referral of venous leg ulcers: lessons from the EVRA trial," *Nurs. Resid. Care*, vol. 22, no. 1, pp. 31–36, 2020.

[4] P. Zhang, J. Lu, Y. Jing, S. Tang, D. Zhu, and Y. Bi, "Global epidemiology of diabetic foot ulceration: a systematic review and meta-analysis," *Ann. Med.*, vol. 49, no. 2, pp. 106–116, 2017.

[5] Z.-Q. Kang and X.-J. Zhai, "The Association between Pre-existing Diabetes Mellitus and Pressure Ulcers in Patients Following Surgery: A Meta-analysis," *Sci. Rep.*, vol. 5, no. 1, pp. 13007, 2015.

[6] B. K. Lal, "Venous ulcers of the lower extremity: Definition, epidemiology, and economic and social burdens," *Semin. Vasc. Surg.*, vol. 28, no. 1, pp. 3–5,. 2015.

[7] J. C. Lawrence, "Wound irrigation," *J. Wound Care*, vol. 6, no. 1, pp. 4, 1997.

[8] A. Gabriel, "Integrated negative pressure wound therapy system with volumetric automated fluid instillation in wounds at risk for compromised healing," *Int. Wound J.*, vol. 9, pp. 25–31, 2012.

[9] N. A. Kantak, R. Mistry, D. E. Varon, and E. G. Halvorson, "Negative Pressure Wound Therapy for Burns," *Clin. Plast. Surg.*, vol. 44, no. 3, pp. 671–677, 2017.

[10] S. Gupta, "Optimal use of negative pressure wound therapy for skin grafts," *Int. Wound J.*, vol. 9, pp. 40–47, 2012.

[11] M. Mir *et al.*, "Synthetic polymeric biomaterials for wound healing: a review," *Prog. Biomater.*, vol. 7, no. 1, pp. 1–21, 2018.

[12] J. Kucińska-Lipka, "Polyurethanes Crosslinked with Poly(vinyl alcohol) as a Slowly-Degradable and Hydrophilic Materials of Potential Use in Regenerative Medicine," *Materials*, vol. 11, no. 3, pp. 352, 2018.

[13] R. R. M. Vogels *et al.*, "Biocompatibility and biomechanical analysis of elastic TPU threads as new suture material," *J. Biomed. Mater. Res. B Appl. Biomater.*, vol. 105, no. 1, pp. 99–106, 2017.
[14] D. Lupuleasa, "biocompatible polymers for 3d printing," *FARMACIA*, vol. 66, no. 5, pp. 737–746, 2018.
[15] A. Krishna, A. Kumar, and R. K. Singh, "Effect of Polyvinyl Alcohol on the Growth, Structure, Morphology, and Electrical Conductivity of Polypyrrole Nanoparticles Synthesized via Microemulsion Polymerization," *ISRN Nanomater.*, vol. 2012, pp. 1–6, 2012.
[16] D. Garcia-Garcia, J. M. Ferri, T. Boronat, J. Lopez-Martinez, and R. Balart, "Processing and characterization of binary poly(hydroxybutyrate) (PHB) and poly(caprolactone) (PCL) blends with improved impact properties," *Polym. Bull.*, vol. 73, no. 12, pp. 3333–3350, 2016.
[17] D. A. Hudson, K. G. Adams, A. Van Huyssteen, R. Martin, and E. M. Huddleston, "Simplified negative pressure wound therapy: clinical evaluation of an ultraportable, no-canister system," *Int. Wound J.*, vol. 12, no. 2, pp. 195–201, 2015.
[18] J. Cantrell *et al.*, "Experimental Characterization of the Mechanical Properties of 3D-Printed ABS and Polycarbonate Parts," *Rapid Prototyp. J.*, vol. 23, no. 4, pp. 811–824, 2017.
[19] T. O. H. Prasetyono, I. S. Rini, and C. Wibisono, "EASEPort NPWT System to Enhance Skin Graft Survival – A Simple Assembly," *Int. Surg.*, vol. 100, no. 3, pp. 518–523, 2015.
[20] V. Milleret, A. G. Bittermann, D. Mayer, and H. Hall, "Analysis of Effective Interconnectivity of DegraPol-foams Designed for Negative Pressure Wound Therapy," *Materials*, vol. 2, no. 1, pp. 292–306, 2009.
[21] M. S. Utomo, Y. Whulanza, F. P. Lestari, A. Erryani, I. Kartika, and N. A. Alief, "Determination of compressive strength of 3D polymeric lattice structure as template in powder metallurgy," *IOP Conf. Ser. Mater. Sci. Eng.*, vol. 541, pp. 012042, 2019.
[22] L. Lu *et al.*, "Mechanical study of polycaprolactone-hydroxyapatite porous scaffolds created by porogen-based solid freeform fabrication method," *J. Appl. Biomater. Funct. Mater.*, vol. 12, no. 3, pp. 145–154, 2014.
[23] H. J. Qi and M. C. Boyce, "Stress–strain behavior of thermoplastic polyurethanes," *Mech. Mater.*, vol. 37, no. 8, pp. 817–839, 2005.
[24] W. Zhang, X. Yang, C. Li, M. Liang, C. Lu, and Y. Deng, "Mechanochemical activation of cellulose and its thermoplastic polyvinyl alcohol ecocomposites with enhanced physicochemical properties," *Carbohydr. Polym.*, vol. 83, no. 1, pp. 257–263, 2011.
[25] F. Chen, D. J. Kang, and J. H. Park, "New measurement method of Poisson's ratio of PVA hydrogels using an optical flow analysis for a digital imaging system," *Meas. Sci. Technol.*, vol. 24, no. 5, 2013.

[26] M. Labet and W. Thielemans, "Synthesis of polycaprolactone: A review," *Chem. Soc. Rev.*, vol. 38, no. 12, pp. 3484–3504, 2009.
[27] M. Al Minnath, G. Unnikrishnan, and E. Purushothaman, "Transport studies of thermoplastic polyurethane/natural rubber (TPU/NR) blends," *J. Membr. Sci.*, vol. 379, no. 1–2, pp. 361–369, 2011.
[28] K. Wahyuningsih, E. S. Iriani, and F. Fahma, "Utilization of Cellulose from Pineapple Leaf Fibers as Nanofiller in Polyvinyl Alcohol-Based Film," *Indones. J. Chem.*, vol. 16, no. 2, p. 181, 2018.
[29] Y. Kanbur and U. Tayfun, "Development of multifunctional polyurethane elastomer composites containing fullerene: Mechanical, damping, thermal, and flammability behaviors," *J. Elastomers Plast.*, vol. 51, no. 3, pp. 262–279, 2019.
[30] V. Goodship and D. K. Jacobs, *Polyvinyl Alcohol: Materials, Processing and Applications*, vol. 16. Shrewsbury, Shropshire: Smithers Rapra Technology, 2009.
[31] M. Sabino *et al.*, "In vitro biocompatibility study of biodegradable polyester scaffolds constructed using Fused Deposition Modeling (FDM)," *IFAC Proc. Vol.*, vol. 46, no. 24, pp. 356–360, 2013.
[32] S. Mohanty *et al.*, "Fabrication of scalable and structured tissue engineering scaffolds using water dissolvable sacrificial 3D printed moulds," *Mater. Sci. Eng. C*, vol. 55, pp. 569–578, 2015.
[33] N. Thuaksuban, R. Pannak, P. Boonyaphiphat, and N. Monmaturapoj, "In vivo biocompatibility and degradation of novel Polycaprolactone-Biphasic Calcium phosphate scaffolds used as a bone substitute," *Biomed. Mater. Eng.*, vol. 29, no. 2, pp. 253–267, 2018.
[34] H. F. Selig, D. B. Lumenta, M. Giretzlehner, M. G. Jeschke, D. Upton, and L. P. Kamolz, "The properties of an 'ideal' burn wound dressing – What do we need in daily clinical practice? Results of a worldwide online survey among burn care specialists," *Burns*, vol. 38, no. 7, pp. 960–966, 2012.